Effects of Mechanical and Chemical Properties on Transport in Fluoropolymers. I. Transient Sorption

SANGWHA LEE[1] and KENT S. KNAEBEL[2]

[1] Department of Chemical Engineering, Kyungwon University, Seongnam City, Korea

[2] Adsorption Research Inc., 6185-D Shamrock Court, Dublin, Ohio, 43016

Received 25 July 1996; accepted 16 August 1996

ABSTRACT: This is the first part of a study of chemical structure-physical property-performance relationships among several fluoropolymers and liquid penetrants, focusing on their diffusivities and solubilities. Transient sorption experiments conducted with perfluoroalkoxy, fluorinated ethylene propylene, and ethylene tetrafluoroethylene exhibited Fickian diffusion. The first two exhibited concentration-independent diffusivity, while the last displayed concentration-dependent diffusivity. Conversely, polyvinylidene fluoride (PVDF) and ethylene chlorotrifluoroethylene (ECTFE) exhibited non-Fickian behavior, including acceleration as saturation approached. Suspected causes for the unusual sorption behavior were structural characteristics due to processing (e.g., skin or orientation with respect to processing direction), intrinsic chemical structure, and morphological deformation induced by swelling. Stress-strain tests indicated that mechanical properties depend similarly on the presence of penetrants to transport properties. Weak swelling agents exhibited Fickian transport and a negligible change of mechanical properties. In contrast, strong swelling agents induced non-Fickian diffusion and caused significant changes of mechanical properties. A new kinetic model fit the transient sorption results, particularly the observed acceleration in PVDF and ECTFE. The model accounts for structural changes due to swelling and relaxation resulting from free-volume creation, which is assumed to be proportional to the amount of liquid sorbed. © 1997 John Wiley & Sons, Inc. J Appl Polym Sci **64:** 455–476, 1997

Key words: sorption; transport; mathematical models; fluoropolymers; properties

INTRODUCTION

Since the discovery of polytetrafluoroethylene (PTFE) by Plunkett in 1938[1] and subsequent commercialization, fluoropolymers have successfully performed in areas that require superior resistance to heat and harsh chemicals. Fluoropolymers can be broadly classified into two major categories: fully fluorinated polymers, e.g., Teflon® PTFE, perfluoroalkoxy (PFA), and fluorinated ethylene propylene (FEP), and partially fluorinated polymers, e.g., Tefzel® ethylene tetrafluoroethylene (ETFE); Hylar®, Kynar®, or Solef® polyvinylidene fluoride (PVDF); and Halar® ethylene chlorotrifluoroethylene (ECTFE). The high strength of the interatomic bonds and the nonpolarity lead to a high degree of crystallinity. This results in beneficial properties such as insolubility, low coefficient of friction, high thermal stability, low permeability, strong chemical resistance, and mechanical toughness.[2]

When some fluorine in a fluorocarbon resin is replaced with hydrogen or chlorine, a distinct change of properties occurs. For example, polarity increases because H and Cl have different electronegativities than fluorine. Accordingly, polarity affects other mechanical and physical properties.

Correspondence to: K. S. Knaebel.

Table I Comparisons of Fully Fluorinated and Partially Fluorinated Polymers

Parameter	Fully Fluorinated Polymers	Partially Fluorinated Polymers
Property	Nonpolarity	Polarity
	Low interchain forces	High interchain forces
	High C—F and C—C bond strength	C—H = 5–10% weak of C—F bond C—Cl = 25% weak of C—F bond
	Relatively high crystallinity (98 ~ 40%)	Relatively low crystallinity (70 ~ 35%)
Benefits	High melting point	High rigidity (1.5 times stiffer than fluorocarbon polymers)
	High thermal stability	
	Inertness to chemical attack	Economical processing

Despite that, characteristics are similar within each group, but there are important differences, as shown in Table I.

Because of their outstanding chemical resistance and low permeability, fluoropolymers are widely used to seal and isolate materials, especially under harsh conditions, in the chemical process industries and in the semiconductor, pharmaceutical, and biotechnology industries, where contamination may be critical.[3–6] Fully fluorinated polymers are used when chemical inertness and high-temperature service are required. Mechanical properties such as creep resistance, stiffness, and toughness have been improved in the 1980s and 1990s.[7] For example, partially fluorinated polymers are better suited to extrusion and injection molding and have greater mechanical strength, but have somewhat lower chemical resistance.

The chemical structures of the fluoropolymers studied here are shown in Figure 1. They are relevant because we attempt to relate structure to transport behavior and mechanical properties. Virgin **PTFE** has an unbranched chain structure and has a crystallinity in the range of 92–98%.

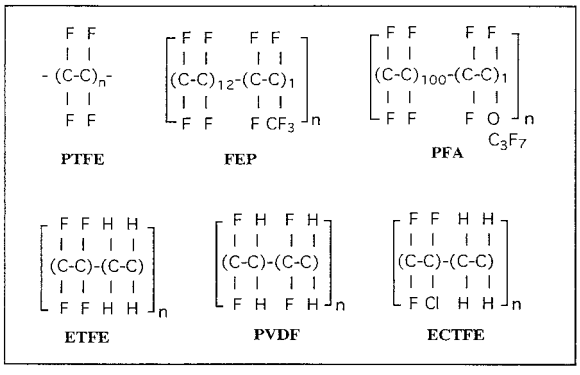

Figure 1 Molecular structures of fluoropolymers.

PTFE has only carbon-carbon bonds, which form the backbone of the polymer chain, and carbon-fluorine bonds.[8] The carbon backbone of the linear chain is completely sheathed by the tightly held electron cloud of fluorine atoms, which shield the carbon chain from chemical attack and confer chemical inertness and stability. It cannot be processed in melt form because chemical decomposition begins below its melting point. At the first-order transition at 30°C, the preferred orientation direction diminishes and the molecular segments oscillate above their long axes with a random angular orientation in the lattice.[9]

PFA is a melt processable copolymer that contains a fluorocarbon backbone in the main chain and a randomly distributed perfluorinated ether side chain ($-OC_3F_7$). The introduction of a perfluorovinyl ether side chain greatly reduces the crystallinity compared with PTFE. **FEP** resin is a copolymer of tetrafluoroethylene and hexafluoropropylene. It retains most of the desirable characteristics of PTFE but has a melt viscosity low enough for conventional melt processing, because perfluoromethyl side groups on the polymer chain reduce crystallinity to 30–45%.

ETFE is isomeric with the homopolymer of PVDF, which is described below. The molecular conformation is an extended zigzag with a nearly perfect alternation of isomeric units in an approximately 1 : 1 monomer ratio. **ECTFE** is another copolymer which essentially alternates in a 1 : 1 ratio of ethylene and chlorotrifluoroethylene. It is partially crystalline, e.g., 50–55%, depending on the method of preparation. The early copolymers were thermally unstable. Thermal stability has been greatly improved by the addition of sterically hindered phenols and other commercially available stabilizers. Polar association occurs between fluorine and hydrogen atoms in this arrangement

and may account in part for the relatively high melting point and the unique properties of the alternating 1 : 1 copolymer.

PVDF is the addition polymer of 1,1-difluoroethene, $CH_2{=}CF_2$. The spatially symmetrical disposition of the hydrogen and fluorine atoms along the polymer chain gives rise to high polarity which can affect solubility and crystal morphology. Crystallinity varies from about 35 to more than 70%, depending on synthesis conditions and thermomechanical history. The glass transition of PVDF apparently lies between −30 and −50°C.[10,11]

The nature of the solution and diffusion of small molecules in polymeric materials can elucidate characteristics such as the flexibility and conformation of chain segments, interactions, free volume change, structural and morphological features, as well as the so-called "molecular probe" aspect.[12] Observations of diffusion in fluoropolymers, however, indicate that the classic theory embodied by Fick's law cannot describe the observed effects adequately in all cases. Depending on the polymer and penetrant, non-Fickian (or anomalous) behavior may appear, sometimes explained via ad hoc or empirical models having limited or no physical basis. In other cases, diffusivity has been viewed as a function of concentration, stress, spatial coordinates, and history of a sample.[13]

The goal of this article is to improve the understanding of fluoropolymers and organic chemicals, relating their chemical structures, physical properties, and mechanical properties, especially as related to transient diffusion, solubility, and tensile strength. A companion article (Part II) presents a similar treatment of fluoropolymer permeability. The common purpose of both parts is to explain test data better so that they can be applied in practical situations. The work presented here is focused on the following polymers: PFA, ETFE, ECTFE, and PVDF with a few sets of FEP, and solvents: benzene, toluene, and chlorobenzene, with a few sets of phenol, methyl ethyl ketone (MEK), and dichloromethane, which were added to explore some specific effects. Other aspects considered are polymer thickness, temperature, orientation, and repeated exposures. The mechanical properties of the fluoropolymers were measured by stress-strain tests and were correlated with the observed transport properties. A kinetic model is used to interpret the transient sorption data. It is based on the assumption that structural changes (e.g., swelling-relaxation effects) associated with sorption can be expressed as free volume change, which is proportional to the amount of liquid sorbed.

THEORY

Background

Three basic classes of transport behavior can be distinguished, depending on the relative contributions of diffusion and relaxation mechanisms[14]:

1. Case I (resembling Fickian diffusion): diffusion is much slower than relaxation.
2. Case II (corresponding to moving front behavior): diffusion is very rapid compared with relaxation, resulting in a moving boundary.
3. Case III (non-Fickian or anomalous diffusion): diffusion and relaxation rates are comparable.

These can be distinguished by the shapes of their sorption curves and, in particular, from the initial fractional mass uptake during sorption, which roughly follows the rate law:

$$F = M_t/M_\infty = kt^n \qquad (1)$$

where k and n are empirical constants. For a Fickian or Case I system, $n = 0.5$ and k is proportional to the diffusion coefficient over the initial half of the sorption experiment. For Case II, $n = 1.0$ and k is directly proportional to the velocity of moving front. For Case III, n usually lies between 0.5 and 1.0.

Non-Fickian transport commonly results from nonlinear dependence and time dependence of transport properties on structural changes associated with sorption. One could think of a "structural diffusivity" as an analogy to structural viscosity in rheology,[15] in the sense that a small degree of structural change can induce a drastic change of diffusivity in polymeric systems. Such is clearly the case in some experiments reported here.

Alternate classifications of non-Fickian sorption phenomena are called anomalies because they do not quite fit expectations. Among them are pseudo-Fickian, sigmoidal, two stage, overshoot, moving front, drastic acceleration, etc. These are briefly described here.

1. *Pseudo-Fickian:* Sorption curves resemble

Fickian curves but show an unusually short initial linear region, i.e., significantly less than 50% of the fractional change. The approach to final equilibrium is also very slow.[16]

2. *Sigmoidal:* Sorption curves often have a single inflection point at about 50% of the equilibrium point. During desorption, the initial rate exceeds that of sorption, but then becomes slower, and the curves cross.[17–19] This is generally observed in differential sorption experiments and may reflect a transition through which distinct sorption characteristics appear: sigmoidal, two stage, and Fickian. Sigmoidal and two-stage (see below) anomalies have been observed by Long and Richman,[20] who attributed them to changes of surface concentration and an outcome of first-order surface relaxation kinetics.
3. *Two stage:* Sorption curves approach a quasi-equilibrium after an initial rapid uptake period, which follows a linear function of the square root of time. The quasi-equilibrium plateau is followed by a slow approach to final equilibrium.[19,21]
4. *Overshoot:* Sorption curves exceed saturation before leveling off at equilibrium.[22–24] Overshoot phenomena involve solvent crystallization within the polymer. The polymer rearrangement and crystallization induced by imbibed solvent adversely affect the sorption process in a minor but detectable manner and eventually repel the sorbed material. Overshoot also occurs as a result of the slow reordering and development of dispersed microvoids within the unrelaxed core, which "heal" as equilibrium approaches.
5. *Moving front:* Uptake is proportional to time (sometimes after an induction period),[25–27] associated with a sharp moving front separating an outer swollen shell from an unpenetrated glassy core. In general, the sorption capacity and the diffusion coefficient of the swollen shell are much larger than in the glassy core, enough to neglect the contribution from the penetration of solvent into the glassy region.
6. *Drastic acceleration:* The rate of uptake increases after a brief initial period, yielding a rapid approach to equilibrium. This is observed during the final stages of sorption envisaged by Jacques et al.[28] as more rapid relaxation, induced by the overlap of precursors ahead of moving fronts, leads to acceleration. They referred to this behavior as super-Case II sorption. To the contrary, Gostoli and Sarti[29] attributed the super-Case II effect to "differential swelling stress," which becomes extremely large as soon as the moving front approaches the midplane. These hypotheses could be tested with samples having one impervious face, e.g., one metallated face and one exposed face.

Sorption Theory

To account for non-Fickian diffusion, others used variable boundary conditions, a modified continuity equation, or both, depending on specific systems and conditions.[30] Crank[14] proposed a model including effects of history, orientation, and stress on both diffusion and surface composition. Our model, however, is based on superimposed diffusion mechanisms.

A separate report fully describes the development of our theory.[31] The material provided here only summarizes that development as necessary to explain results. Following Berens and Hopfenberg,[32] we split the fractional uptake during transient sorption into two additive parts: one due to Fickian diffusion, F_F, and the other due to relaxation, F_R, with relative weights of $(1 - \alpha)$ and α, respectively.

$$F = (1 - \alpha)F_F + \alpha F_R \tag{2}$$

We also kept the Fickian portion as the solution for one-dimensional diffusion in a slab with constant boundary conditions and a constant diffusivity, D_F.

$$F_F = 1 - \sum_{n=0}^{\infty} \frac{8}{(2n + 1)^2\pi^2} \times \exp(-D_F(2n + 1)^2\pi^2 t/l^2) \tag{3}$$

Relaxation is often associated with changes of free volume, as suggested by Doolittle,[33] Williams et al.,[34] and Fujita.[35] It corresponds to structural changes, such as swelling, microcavity formation, etc., with a corresponding volume change, ΔV, proportional to the amount of material sorbed. The fractional volume change due to relaxation

effects is assumed to be equal to the fractional uptake (or release) as follows:

$$F_R = \frac{M_R}{M_{R\infty}} = \frac{C_f - C_{f0}}{C_{f\infty} - C_{f0}} = \frac{f - f_o}{f_\infty - f_o} = \frac{v}{v_\infty} = \frac{\Delta V}{\Delta V_\infty} = \frac{V - V_0}{V_\infty - V_0} \quad (4)$$

where f is the fractional free volume defined in Fujita's free-volume theory, and v is the volume fraction of the penetrant, assuming constant partial molar volumes. It is evident that the rate of free volume change is the same as that of the specific volume according to Fujita's free-volume theory. If the amount of sorbed material is low (e.g., less than $10 \sim 15$ vol %), the volume fraction of penetrant can be slightly modified into a simple form below.

$$v = \frac{\Delta V/V_o}{1 + \Delta V/V_o} \simeq \frac{\Delta V}{V_o} \quad (5)$$

The rate of accumulation of the penetrant due to structural change is assumed to be proportional to $1 - F_R$, the fraction that is still unoccupied, via a pseudo-first-order mechanism:

$$1 - F_R \overset{k_f}{\rightharpoonup} F_R \quad (6)$$

$$\frac{dF_R}{dt} = k_f(1 - F_R) \quad (7)$$

The rate coefficient, k_f, apparently depends on penetrant concentration because it has been observed that higher concentrations of penetrant produce faster rates of structural change.

Exponential-Dependence Rate Equation

First, a simple exponential function is proposed, relating the diffusion coefficient and rate constant to the penetrant volume fraction.

$$k_f = k_{f0}\exp(\gamma_k v) \quad (8)$$

In view of eq. (4), the free volume in eq. (8) can be replaced: $k_f = k_{f0}\exp(K'F_R)$, where $K' = \gamma_k v_\infty = K \log_e(D_\infty/D_0)$ [see eq. (11) below)], and where $K = \gamma_k/\gamma_D$. The resulting rate equation is:

$$\frac{dF_R}{dt} = k_{fo}\exp(K'F_R)(1 - F_R) \quad (9)$$

This is referred to below as the exponential rate equation, denoting its dependence on sorption due to relaxation. The following four parameters are adjusted to fit experimental data:

1. α = Fraction of total uptake that occupies the newly created free volume.
2. D_F (cm^2/day) = Fickian diffusivity or intrinsic diffusivity.
3. k_{f0} (1/day) = Relaxation rate coefficient.
4. γ_k (cm^3/g) = Sensitivity coefficient of the relaxation rate parameter.

Quadratic-Dependence Rate Equation

An alternate rate equation was obtained by postulating that the rate parameters were dependent on the polymer free volume, f, following the approach of Williams et al.[34] and Doolittle.[33] Their relation is:

$$D = RTA_d\exp(-B_d/f) \quad (10)$$

Following their approach yields a simple expression for the rate constant:

$$k_f = k_{f0}(D/D_0) \quad (11)$$

The diffusivity ratio, D/D_0, can be reduced to a simple exponential form and further to linear form if the free volume increment is small compared with the amount of initial free volume (as for most fluoropolymers), via a Taylor's series expansion of eq. (10).[36]

$$D = D_0(1 + \gamma_D v), \quad \text{for } \gamma_D v \leq 0.3, \quad \text{where } \gamma_D = \frac{B_d\gamma}{f_0^2} \quad (12)$$

where $\gamma_D = B_d\gamma/f_0^2$ is a parameter suggested in the Williams et al. (WLF)-Doolittle approach.

In this case, a new F_R relationship can be obtained in terms of diffusion coefficients, and the rate coefficient turns out to be linearly dependent on the concentration of the penetrant.

$$F_R = \frac{\Delta V}{\Delta V_\infty} = \frac{v}{v_\infty} = \frac{D - D_0}{D_\infty - D_0} \quad (13)$$

$$k_f = k_{f0}([D_\infty/D_0 - 1]F_R + 1) \quad (14)$$

When eq. (14) is inserted into the rate eq. (7) and integrated, the following expression is obtained:

$$F_R = \frac{1 - \exp(-k_{f_o}\epsilon t)}{1 + (\epsilon - 1)\exp(-k_{f_o}\epsilon t)} \qquad (15)$$

For the quadratic rate equation, there are also four adjustable parameters:

1. α = Fraction of total uptake that occupies the newly created free volume.
2. D_F (cm^2/day) = Fickian diffusivity or intrinsic diffusivity.
3. k_{fo} (1/day) = Relaxation rate coefficient.
4. ϵ = Diffusivity ratio, D_∞/D_0.

The value of D_F can be obtained from the initial slope of the sorption curve based on Fickian response. The fraction, α, must be assessed simultaneously. So, this value should be reevaluated considering the total mass uptake[28]: $D_0 = D_F(1 - \alpha)^2$.

Subsequently, eqs. (9) and (15) will be compared with actual sorption rate data. The parameters' values determined from those comparisons are then used to explain the behavior of the polymer and the penetrant.

To validate the mechanisms and measured solubility and diffusion parameters, permeation rates were calculated from the fitted parameters and compared with steady-state permeation data with the some materials as used here.[37] In particular, the sorption kinetics of FEP and PFA are described by simple Fickian diffusion with a constant diffusion coefficient. For steady-state permeation through a polymer sheet without conveyance effects, the rate of flux is given by:

$$J_A = -D\frac{dC}{dx} = D\frac{C_1 - C_2}{l} \qquad (16)$$

where l is the thickness of the sample, and C_1 and C_2 are the surface concentrations of component A in the polymer on the upstream and downstream sides, respectively. The latter is commonly exposed to air and is usually nil. Thus, the diffusivity from the Fickian diffusion equation combined with the solubility can predict the permeation rate. Similarly, the flux equation corresponding to eq. (15) can be derived:

$$J_A = \frac{D_o}{\gamma_D l}(\exp(\gamma_D C) - 1) = \frac{D_o(D_\infty/D_o - 1)}{\ln(D_\infty/D_o)}\frac{C_\infty}{l} \qquad (17)$$

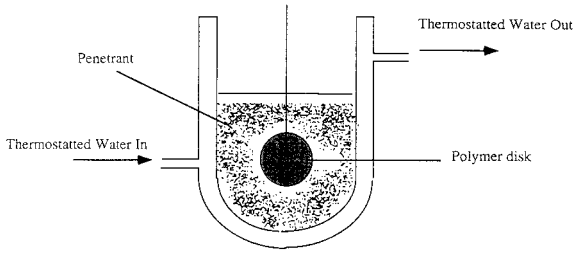

Figure 2 Jacketed apparatus for measuring liquid sorption rates.

Permeation rates were calculated by the use of eq. (16) or (17) and were compared with experimental data.

EXPERIMENTAL METHODS AND CONDITIONS

Transient Sorption

Transient sorption experiments were conducted to determine both the effective diffusivity and the solubility of the penetrant in the polymer. Variables that were systematically tested include: the thickness of the sample (0.25 and 2.3 mm), temperature (25, 45, and 65°C), and the penetrants (aromatic liquids and some hydrocarbon solvents). Several fluoropolymers were tested: ETFE, ECTFE, PVDF, PFA, and FEP. Three replicates of each experiment were completed. These involved a preweighed and measured polymer disk (7.62 cm diameter) that was suspended on a wire and immersed in a pure penetrant liquid contained in a jacketed flask, of which temperature was controlled by circulating water through the jacket. The sample was removed, blotted dry, and then weighed at certain intervals. A schematic diagram of the apparatus is shown in Figure 2. A balance with an accuracy of ±0.1 mg was used to measure the mass change of the immersed polymer films. The dimensions of each sorbed sample were also measured periodically with digital calipers (sensitivity = ±0.025 mm). Vapor-phase sorption experiments were also performed, but only at 45°C. The vapor composition was set by flowing the carrier gas (dry air) through a thermostatted liquid solvent reservoir.

Corresponding rate data were interpreted via the solution to an "Initial Value Problem." That is, the effective diffusivity was obtained from transient sorption experiments, using the solution of the governing partial differential equation,

as outlined earlier. Likewise, the solubility was measured by allowing a preweighed sample to remain in contact with the penetrant for an extended period, weighing it repeatedly, and denoting the steady-state value as equilibrium.

Stress-Strain Tests

Stress-strain tests were conducted at 25°C, before and after immersion in various penetrants. Besides categorizing their inherent mechanical properties, our purpose in stress-strain testing was to understand the effects of penetrants on the polymer mechanical properties, e.g., strength or toughness, and the relationship between the observed transient sorption behavior of penetrants with their effect on mechanical properties. Two properties were measured: tensile stress and tensile strain, which are important indicators of the strength of a material, as explained in more detail below.

These were conducted with a Tensometer model 20 (Monsanto, Serial No. ST20-136), which measured the applied tensile force and the resulting extension of the sample in accordance with major international standards. The movable crosshead moved at a constant rate (50.5 cm/min). Stress was automatically plotted versus strain. Numerical values of stress and strain were also recorded manually from a digital readout on the machine. Each specimen was prepared by cutting a sample sheet into a 14-cm-long by 1.3-cm-wide-necked tensile bar. Each of these had 2.5-cm-wide ends that were clamped in the crossheads.

There are usually four regions observed during stress-strain testing: elastic, yield, draw region with neck, and postneck region.[38] Below the yield point, elastic deformation occurs and the initial slope is the Young's modulus, a measure of stiffness. The yield point coincides with permanent deformation or neck formation, identified by a zero slope on the stress-strain curve. After neck formation, the stress drops to a lower yield load. In the subsequent draw region, an almost constant load propagates through the sample and typically transforms the original glassy structure into a highly oriented fibrous structure, accompanying strain hardening, reflecting an increase of the modulus and tensile strength. Finally, the sample breaks, although this rarely occurred in our trials because of the limited range of the Tensometer.

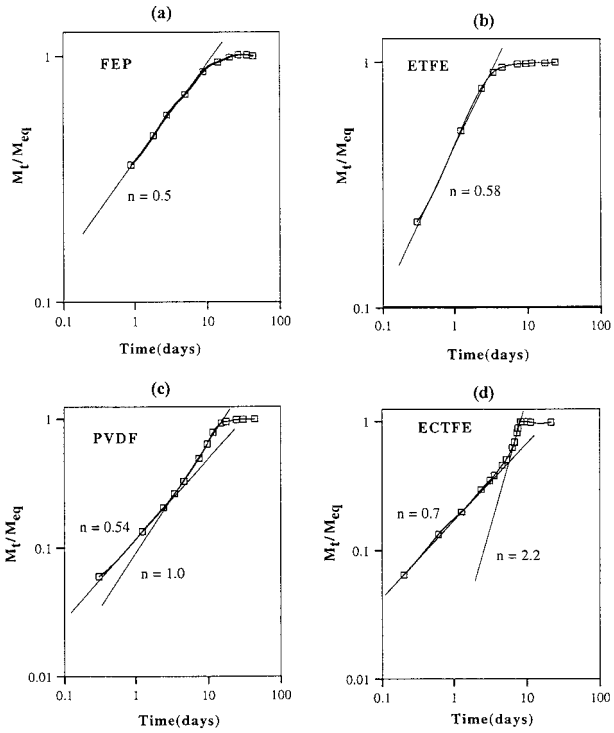

Figure 3 Log-log plots of the kinetics of benzene sorption by fluoropolymers at 25°C (n = slope of log-log plot). Note: if not specified in the following figures, the thickness of the polymer samples is 0.25 mm.

EXPERIMENTAL RESULTS AND DISCUSSION

Sorption Characteristics

For the transient sorption experiments, the range of responses spanned from Fickian, with either concentration-independent or concentration-dependent diffusivity, to various forms of non-Fickian behavior, some of which exhibited acceleration during the final stages of uptake. Applying eq. (1) allows us to classify the rate of sorption among the types of polymers. FEP and ETFE films [as shown in Fig. 3(a) and (b)] exhibited slopes of approximately 0.5 for the sorption of benzene up to about 70%, which is characteristic of Fickian diffusion and Case I sorption. The slope for PVDF, however, rises from about 0.5 to 1.0 [as shown in Fig. 3(c)]. This observation indicates that relaxation effects contribute to the total sorption uptake along with concentration-driven Fickian diffusion, corresponding to Case III sorption. ECTFE exhibited a slope of about 2.2 during the final stage of uptake (i.e., $M_t/M_\infty \propto t^{2.2}$) [as shown in Fig. 3(d)], which corresponds to drastic acceleration. This exponent is greater than others re-

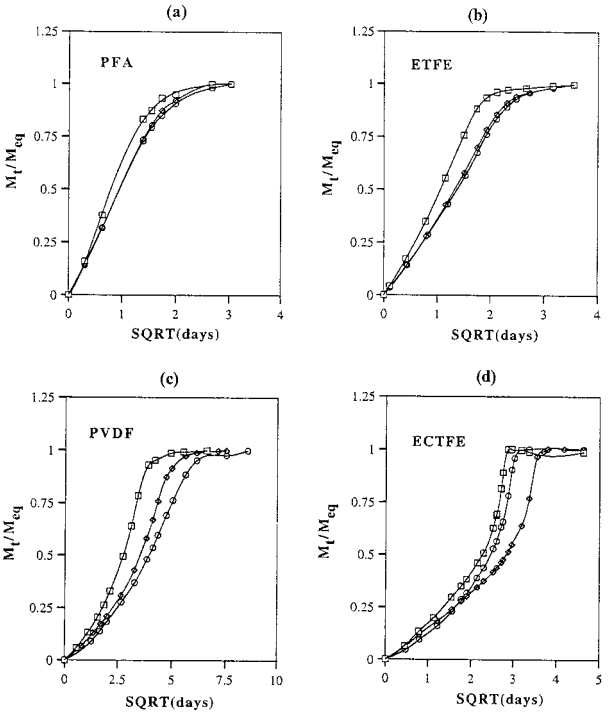

Figure 4 Integral sorption of aromatic liquids into fluoropolymers at 25°C. (□) benzene, (◇) toluene, (○) chlorobenzene. Curves are simply spline fits of the data.

ported previously. The discussion below examines the causes and effects in greater detail. The factors discussed are different polymer and penetrant types, effects of repeated exposure, processing conditions (orientation, thickness, and skin), and plasticization.

Solvent and Polymer Types

Homologous aromatic solvents (benzene, toluene, and chlorobenzene) were used as penetrants. It was found that nonpolar solvents penetrated faster through nonpolar fluoropolymers than did polar solvents, and vice versa. Furthermore, for the same polarity, smaller molecules penetrated faster than larger ones. Solubility followed the same general trends. For example, because of its small size, benzene exhibited the highest solubility in all of the fluoropolymers among the homologous series. In addition, Figure 4(a) through (c) show that nonpolar benzene and toluene penetrated faster than polar chlorobenzene and that smaller benzene penetrated faster than larger toluene in PFA, ETFE, and PVDF, which are known to be nonpolar. That figure shows fractional uptake versus square root of time (in days$^{0.5}$). In addition, as shown in Table II, nonpolar benzene and toluene exhibited high solubility in ETFE and PVDF. Conversely, the more polar ECTFE was more susceptible to polar solvents, as shown in Figure 4(d), i.e., chlorobenzene was faster than toluene. Likewise, again as shown in Table II, chlorobenzene exhibited higher solubility in ECTFE than did toluene. Likewise, its solubility was higher by about 70% in ECTFE than in either ETFE or PVDF.

Solvents with strong H-bonding ability such as MEK and phenol affected PVDF to a much greater extent than ETFE or ECTFE. In contrast, the sorption of phenol by PFA and ECTFE was observed to be nil at 25°C. Furthermore, Table II indicates that the solubilities increased by approximately 0.5 to 1.0%/K from 25 to 65°C, following a van't Hoff type of relationship. The energies of sorption (ΔH_s) turned out to be small and positive, as shown in Table III.

FEP exhibited nearly Fickian sorption and desorption behavior with a constant diffusivity. Both reduced curves roughly coincided with each other over the entire range of the experimental time scale, as shown in Figure 5(a). When viewed on "fractional mass change" versus "square root of time" coordinates, the data were initially roughly linear and then approached saturation asymptotically, in congruence with Fick's law. The diffusion coefficient thus can be obtained from eq. (3).

Similarly, ETFE exhibited slightly distorted Fickian sorption behavior. There was a slight inflection at the outset of sorption, as shown in Figure 5(b). In addition, as shown in that figure, the desorption curve is slightly above the sorption curve over the initial half of the sorption curve, and then the curves cross, which violates the strict assumptions of Fick's law. Nevertheless, the effective diffusivity of ETFE can be represented as concentration dependent, and a suitable value for uptake, D_u, or release, D_r, can be estimated from the respective average value of the initial gradient by assuming that Fick's law is valid. The extent of deviation from Fick's law was very small compared with ECTFE and PVDF, possibly because the polymer structure is more uniform and there is no apparent skin. Moreover, the strength of interchain interactions may be so weak that relaxation effects were minimal. In summary, the seemingly Fickian sorption in ETFE resins results from minor relaxation-controlled structural change due to small free-volume creation, or possibly due to the time scale of relaxation being

Table II Solubilities of Solvents in Polymers at 25, 45, and 65°C

Polymer	Temperature (°C)	Solubility (mol [penetrant]/cm^3 [polymer]) $\times 10^4$		
		Benzene	Toluene	Chlorobenzene
ETFE	25.0	5.21	3.99	3.80
	45.0	5.74	4.25	4.10
	65.0	6.77	4.84	4.56
ECTFE	25.0	7.43	5.68	6.25
	45.0	8.30	6.18	6.85
	65.0	10.79	7.49	7.92
PVDF	25.0	5.59	4.05	3.33
	45.0	6.20	4.53	3.79
	65.0	7.28	5.16	4.36

short enough to neglect relaxation effects on diffusion.

PVDF film produced a sigmoidal sorption curve with a single inflection point, as shown in Figure 5(c) for benzene. After a short linear period, the curve became convex with respect to the time axis, indicating that uptake was accelerating. Afterwards, the curve approached saturation asymptotically. The reduced desorption curve apparently intersected the sorption curve and approached the final state very slowly, compared with uptake. The magnitude of effect varied among the solvents, and to explain their effects, they are divided into three types: 1) nonplasticizing (phenol or benzene vapor), 2) slightly plasticizing (liquid benzene, toluene, and chlorobenzene), and 3) highly plasticizing (MEK and dichloromethane). For solvents of type 1, a slight inflection was observed in the sorption curves. The inflection indicated that a slight structural change occurred during diffusion. For solvents of type 2, the observed sorption curve exhibited sigmoidal shapes, followed by an asymptotic approach to the final equilibrium uptake. For solvents of type 3, the sorption behavior resembled that of ECTFE, except acceleration abated during the final approach to equilibrium.

PVDF did not exhibit the characteristics of a tough skin, even when samples had a shiny surface. That is, there was no significant distortion (or curling) during sorption. It was also observed that the longitudinal expansion of PVDF was linearly dependent on mass uptake, as shown in Figure 6(a). The characteristics due to orientation

Table III Sorption Energies from Clapeyron-Type Plots (Ln [Solubility] Versus Temperature^{-1} [K^{-1}])

Polymer	Sorption Energy, ΔH_s (kcal/mol)		
	Benzene	Toluene	Chlorobenzene
ETFE	1.302	0.955	0.908
ECTFE	1.848	1.372	1.178
PVDF	1.314	1.201	1.346

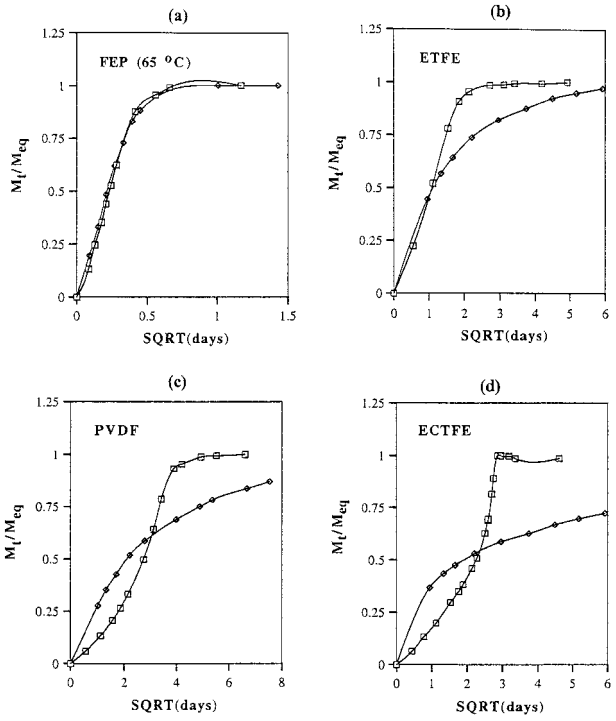

Figure 5 Integral sorption and desorption of benzene in fluoropolymers at 25°C, except FEP, which is at 65°C. Film thickness is 0.25 mm. (□) sorption, (◇) desorption.

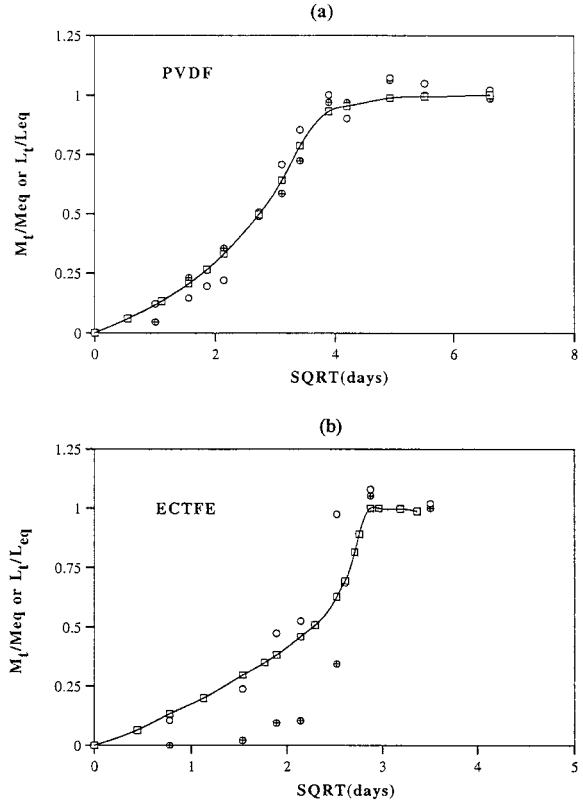

Figure 6 Time dependence of integral sorption and specimen length for benzene penetration in PVDF and ECTFE at 25°C. (□) sorption curve, (⊕) expansion in the machine direction, (○) expansion in the transverse direction.

in the machine direction were not clearly observed in PVDF. The ratio of expansion in the (inferred) machine direction to that of the (inferred) transverse direction was, however, about 2.

The underlying cause of the behavior exhibited by PVDF was due to its greater H-bonding characteristics. In general, H bonding is stronger and more localized at the interaction sites, compared with dipole-dipole interactions. Therefore, the disruption of one interchain bond may be much less influential on the neighboring interaction sites (in contrast to ECTFE, as explained below). Thus, the sorption behavior of PVDF was mainly affected by the degree and strength of interactions between polymers and penetrants, not by a structural factors due to chemical composition or processing conditions, as for ECTFE.

ECTFE film produced even more unusual results than the other polymers, as shown in Figure 5. Sorption curves exhibited essentially no linear region but were immediately convex with respect to time, indicating greater acceleration of uptake than PVDF. Finally, instead of approaching saturation asymptotically, the sorption rate appeared to accelerate until saturation was attained or sometimes exceeded slightly. This acceleration feature cannot be described by a linear combination of Fickian and Case II relaxation effects, e.g., as in eq. (2). In ECTFE, the rapid relaxation as saturation is approached led to accelerating uptake of solvent with accompanying rapid expansion in the machine direction. This type of behavior was first reported for the sorption of n-hexane by polystyrene by Jacques et al.[28] as super Case II sorption, which is an extreme outcome of Case II sorption kinetics. There are, however, some factors that favor our continuous relaxation mechanism rather than the moving front concept, viz., fluoropolymers exhibit low sorbed concentration, no craze or cracks, and low relative sensitivity to temperature, thickness, and penetrant types. Instead, we believe other morphological features (e.g., characteristics imbued by processing [such as roll coating], orientation, and intrinsic chemical structure) may cause acceleration during sorption.

ECTFE has intersegmental dipole-dipole bonds, due to balanced electronegativities between chains. It is believed that the stiff ECTFE chains are oriented in parallel arrays, maximizing the accessibility of substituent groups to interchain polar attraction, such that the disruption of one of these bonds in a set of parallel chains (e.g., by one polar solvent molecule) facilitates the disruption of other bonds, as in unzipping a zipper. Ultimately, the disruption of bonds increases exponentially as sorption proceeds, resulting in greater mobility for the polymer molecules and leading to accelerated uptake during the final stage of sorption.

The main cause of non-Fickian diffusion in partially fluorinated polymers seems to arise from hydrogen bonding and polar interchain attractions caused by substituent elements. As fluorine atoms are replaced by hydrogen, the substituted hydrogen atoms become increasingly electrophilic in nature. The reason is that the fluorine atom has a strong electron-withdrawing power, resulting in a decrease in electron density around the carbon atom that is compensated, in part, by a shift of the electrons away from the hydrogen, increasing the acidic character of that hydrogen atom. Thus, a 1 : 1 random head-to-head type of copolymer of tetrafluoroethylene and ethylene (ETFE) is much less reactive toward H-bonding solvents than is the head-to-tail type (PVDF), yet their elemental

analyses are identical. In this case, the hydrogen in ETFE (which is bonded to a carbon atom that is adjacent to only one carbon carrying fluorine) is less electrophilic than the counterpart hydrogen in PVDF. In ECTFE, on the other hand, a fluorine atom is replaced by a chlorine atom, which has less electron-withdrawing power than fluorine. The chlorine atom disturbs the electronic balance within intrachain segments but hardly affects the acidic character of neighboring hydrogens. As a result, dipole-dipole interactions between interchain segments in ECTFE increase.

Actually, sorption experiments with vapor-phase benzene indicated that PVDF and ECTFE were more effective barriers than PFA or ETFE. The times required to achieve 99% saturation for liquid-phase benzene versus vapor-phase benzene were: 0.6 versus 2.5 days for PFA and 0.8 versus 7.3 days for ETFE, but 1.2 versus 11.6 days for PVDF and 0.4 versus 56 days for ECTFE. At high penetrant activity, however, the segmental mobility in partially fluorinated polymers increases because of the disruption of polar intersegmental bonds, probably as a result of the plasticization effects of highly swelling penetrants. Consequently, these polar polymers become more vulnerable to the attack of liquid-phase solvents. In addition, the creation of free volume due to the disruption of intersegmental bonds may induce the time dependence of both diffusivity and solubility.

Effects of Processing Properties: Nonisotropic Expansion

Thickness changes due to immersion in aromatic solvents were difficult to detect accurately, because of the small variations and because the polymer was slightly compressible. Conversely, shape changes (or deformations) were evident in ECTFE film because of the existence of a tough, shiny skin on one side and a relatively soft, dull surface on the other side. During sorption, the dull side expanded more than the shiny side, which caused the polymer to curl toward the shiny side. None of the other polymers exhibited significant skin differences or shape changes. Longitudinal swelling (or linear expansion) of ETFE and PVDF was observed to be fairly small (e.g., on the order of 1–2%) and isotropic. PVDF expanded more in the (inferred) machine direction than in the transverse direction [see Fig. 6(a)], while ETFE showed the opposite response. ECTFE, on the other hand, swelled to a much greater extent, e.g., by 3–5% in the machine direction. Conversely, it only exhibited minor expansion ($\sim 1\%$) in the transverse direction. The swelling was not symmetric: expansion in the transverse direction followed the fractional uptake consistently, but the expansion in the machine direction lagged and then, above a certain fractional mass uptake, increased rapidly. This appeared to be a result of swelling stress, possibly caused by the more expandable dull side. As shown in Table IV, there were no systematic effects of temperature or differences among the solvents on the degree of expansion of a given fluoropolymer.

Analysis of Mathematical Models

Fickian Diffusion

For Fickian sorption behavior, sorption rate data are analyzed via eq. (2), as discussed by Crank.[14] A test of the validity of this method lies in the ability to combine the diffusivity and solubility measured in sorption experiments and to compare them with steady-state permeation rates. Accordingly, permeation rates calculated from measured values of diffusivity and solubility for FEP with benzene at 25 and 45°C are compared with corresponding experimentally measured permeation rates, as shown in Table V. The discrepancies are only about 10%, which is remarkably good. This confirms the validity of Fick's law for the transport of organic liquids in FEP. PFA also exhibits almost perfect Fickian behavior (except at 45°C, which shows slight sigmoidal behavior), as shown in Figure 7.

Non-Fickian Diffusion

ETFE exhibits concentration-dependent sorption behavior, e.g., varying diffusivities and slight relaxation effects. Therefore, the surface concentration may be described by first-order relaxation kinetics, as by Long and Richman.[20] For this case, the continuity equation with a concentration-dependent diffusivity and a time-dependent boundary condition can predict the sorption behavior of ETFE with adjustable parameters such as initial surface concentration, surface relaxation coefficient, and plasticizing diffusion coefficient. Ignoring the effect of surface relaxation, the sorption curves of ETFE can also be approximated by Fick's equation with a concentration-dependent diffusivity, as explained in the prior section.

The sorption behavior of PVDF and ECTFE was analyzed by the kinetic models presented ear-

Table IV Equilibrium Expansion of Polymers 0.25 mm (10 mil = 0.010 in.) Thick after Immersion in Penetrants[a]

Penetrant	Temperature (°C)	Orientation	Expansion of Polymer (%) ETFE	ECTFE	PVDF
Benzene	25	Transverse	1.2	0.93	1.2
		Machine	0.93	3.5	2.2
	45	Transverse	1.5	1.1	1.4
		Machine	0.30	3.5	2.4
	65	Transverse	1.4	1.2	1.3
		Machine	0.27	4.8	2.9
Toluene	25	Transverse	1.3	0.93	1.2
		Machine	0.93	3.0	2.0
	45	Transverse	1.3	0.87	1.1
		Machine	0.57	3.5	2.2
	65	Transverse	1.07	0.93	1.3
		Machine	−0.07	4.13	2.1
Chlorobenzene	25	Transverse	1.2	1.1	0.83
		Machine	0.08	3.2	1.5
	45	Transverse	1.3	0.73	0.87
		Machine	0.2	3.3	1.4
	65	Transverse	1.0	1.2	1.2
		Machine	0.23	4.5	1.9

[a] If not specified in the following tables, the thickness of the polymer samples is 0.25 mm.

lier. The acceleration exhibited by ECTFE was in good agreement with the exponential type of rate expression that was given by eq. (9), as shown in Figure 8. Table VI lists the fitted parameters and shows that the amount of uptake due to relaxation, α, was about 0.6–0.7. The initial diffusivity and relaxation coefficient both increased by a factor of 20 as the temperature increased by 20°C. The relaxation sensitivity coefficient, γ_k, decreased as temperature increased. This indicates that relaxation effects decrease as the temperature increases, possibly because relaxation has a higher apparent activation energy than diffusion. Similarly, in previous studies of Case II sorption, the mechanism was observed to change from relaxation-controlled diffusion to diffusion-limited relaxation (or Fickian diffusion) as temperature increased.[39–41]

For the exponential rate equation, it is not straightforward to predict permeation rates with only fitted parameter values from sorption rate experiments. In particular, the parameter K' or γ_k in eq. (9) and the ratio D_∞/D_0 are so closely related that these two values cannot be obtained independently by curve fitting. To compare theoretical permeation rates from this model versus experimental data, e.g., for ECTFE, the value of γ_D should be determined via a series of differential sorption experiments or from permeation rate data itself. In this approach, γ_D was roughly estimated from eq. (17) with known C_∞, l, and fitted D_0 values. The fitted D_∞/D_0 value from the four-

Table V Comparison of Calculated Permeation Rates with Experimental Results for the FEP-Benzene System

Temperature (°C)	Calculated Values[a] Solubility	Diffusivity	Flux	Experimental Flux
25	0.0079	0.14E-04	0.0484	0.0443
45	0.0094	1.03E-04	0.4227	0.4717

[a] Units: solubility (g/cm^3), diffusivity (cm^2/day), flux ($g/m^2 \cdot day$).

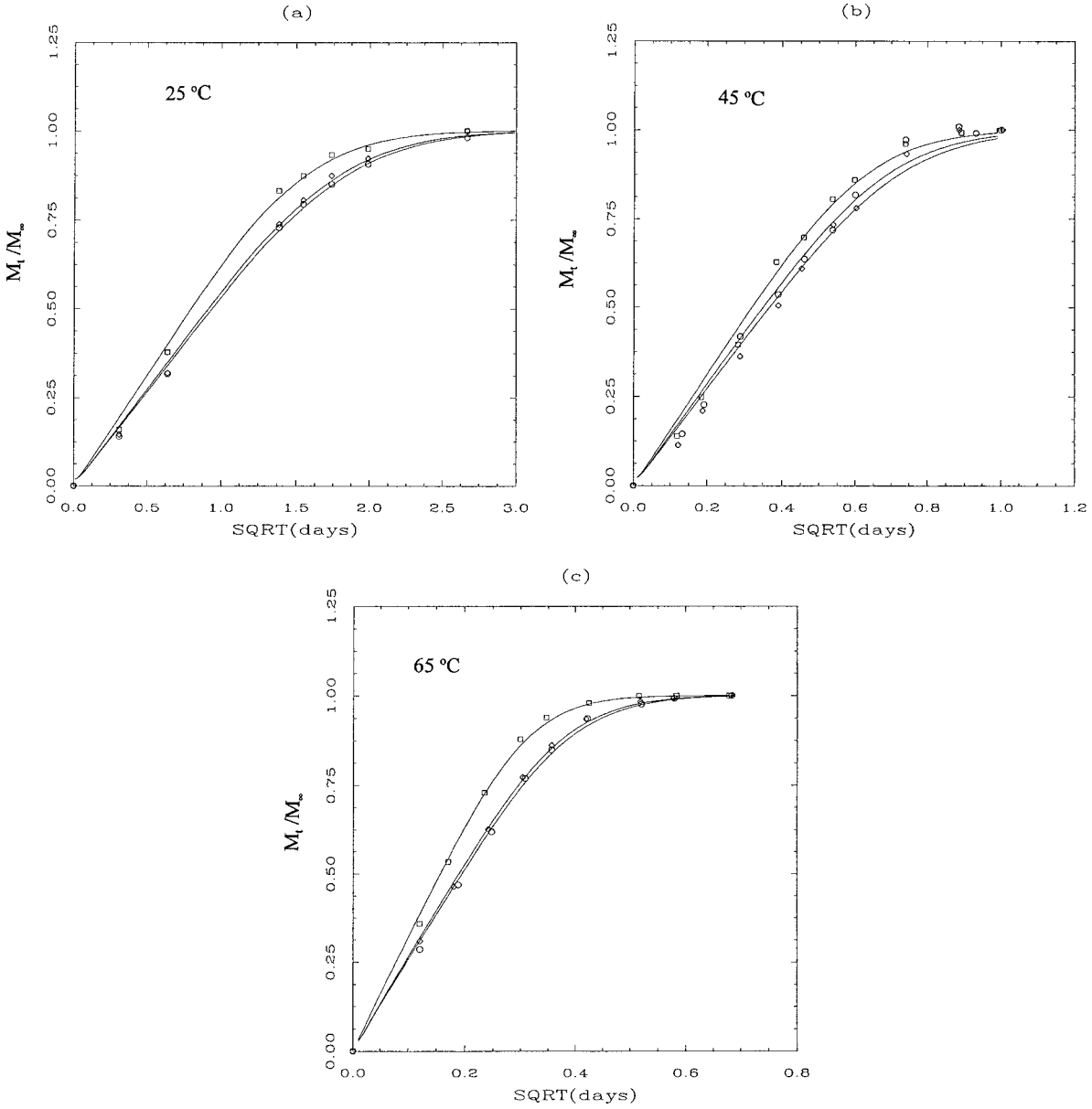

Figure 7 The fitted data of PFA with liquid toluene sorption at 25, 45, and 65°C by simple Fickian equation. (□) benzene, (◇) toluene, (○) chlorobenzene.

parameter exponential model, eq. (9), was again used to predict permeation rate with the use of eq. (17). As summarized in Table VII, deviations from experimental data were within an average of 5%. The result clearly indicates that the exponential model is quite compatible with the flux equation, having exponential dependence of diffusivity on concentration.

This model equation was extended to interpret the anomalous sorption curves observed for ECTFE films. For example, the initial diffusion coefficient, D_o, in repeatedly exposed samples appears to be consistently smaller than that of fresh samples, on the basis of the experimental observations. Likewise, the relaxation fraction, α, in presorbed samples also appears to be consistently larger than that of fresh samples. The fitted values match well with the data and are summarized in Table VIII. The fitted curves and data are also shown in Figures 9 and 10.

On the other hand, the sigmoidal sorption curve of PVDF was in good agreement with the quadratic rate expression that was given by eq. (15). The values listed in Table IX represent the

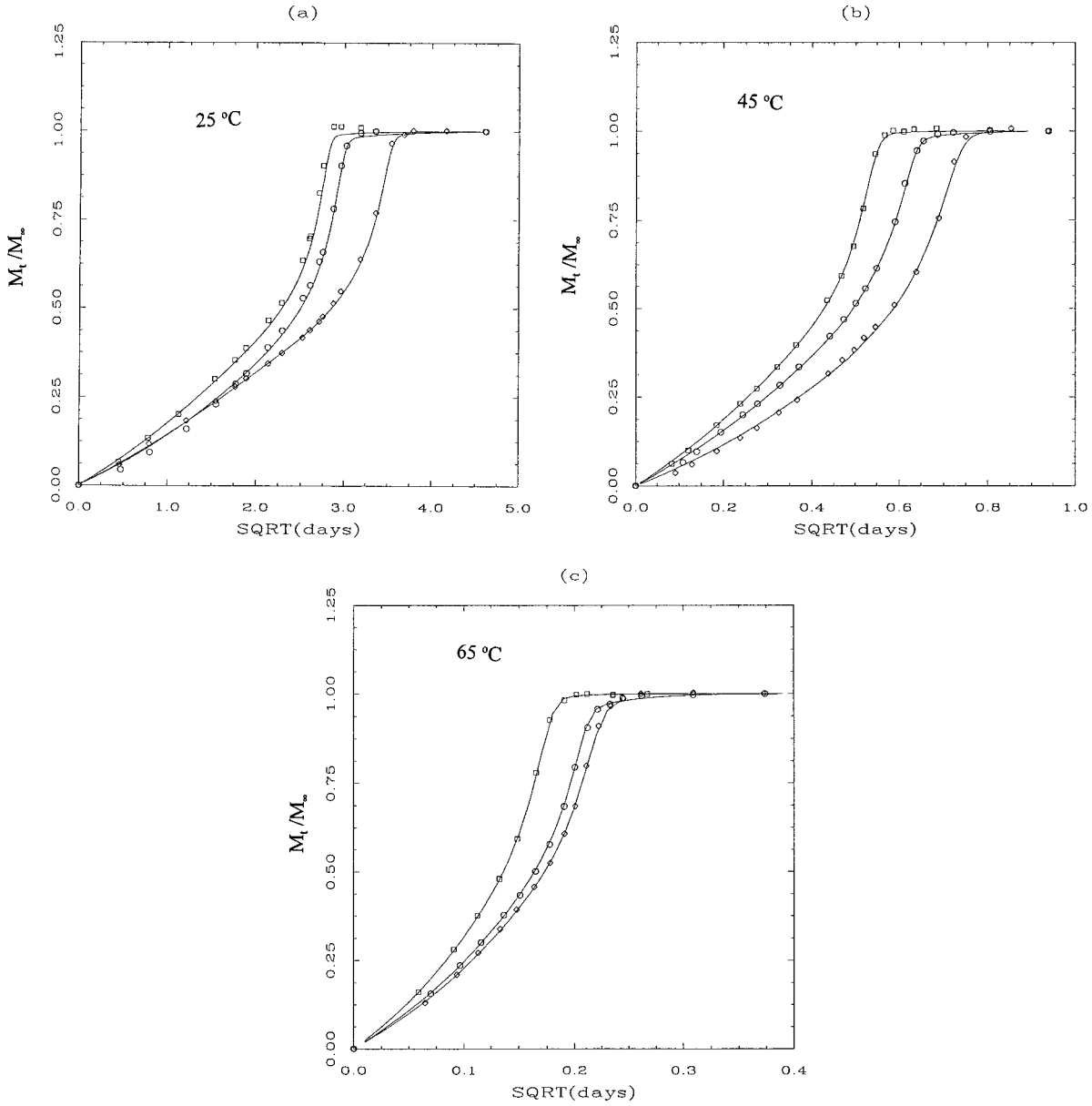

Figure 8 The fitted data of ECTFE with aromatic liquid sorption at 25, 45, and 65°C by an exponential type of rate equation. (□) benzene, (◇) toluene, (○) chlorobenzene.

observed sorption curves for PVDF quite well, as shown in Figure 11. As temperature increases, both the initial diffusivity, D_o, and the relaxation rate coefficient, k_{fo}, increase. Regardless of temperature, the amount of uptake due to relaxation, α, is about 0.7–0.8. Permeation rates were calculated via eq. (17) with parameters from transient sorption experiments, i.e., without iterating, and were compared with experimental data in Figure 12 and Table X. The deviations from experimental data were within ±30% except for benzene, for which the experimental values were about 50% less than the predicted permeation rates. The result indicates that permeation rates can be predicted from fitted parameters for transient sorption, with modest discrepancies. Thus, the quadratic rate equation is at least partially validated because it represents these diverse modes of transport consistently.

Finally, the rate parameters, D_o and k_{fo}, obtained from Tables VI and IX, are plotted as in the Arrhenius relationship in Figure 13. The panels show that the relationship was linear over the limited range tested. The approximate activation

Table VI Fitted Rate Parameters for Sorption Rate Experiments via Eq. (9) for Various Penetrants in ECTFE

Temperature (°C)	Parameter	Fitted Parameter Values for ECTFE		
		Benzene	Toluene	Chlorobenzene
25	α	0.656	0.643	0.678
	$D_o \times 10^4$	0.0245	0.0177	0.0151
	k_{fo}	0.0325	0.0201	0.0295
	γ_k	90	101	72
45	α	0.678	0.734	0.632
	$D_o \times 10^4$	0.625	0.244	0.472
	k_{fo}	1.06	0.609	0.771
	γ_k	68	76	58
65	α	0.675	0.675	0.607
	$D_o \times 10^4$	5.28	3.094	3.83
	k_{fo}	11.4	7.21	7.59
	γ_k	47	59	47

Table VII Calculated Permeation Rates from Fitted Parameters of the Exponential Rate Equation and Experimental Values for Various ECTFE-Penetrant Systems

Temperature (°C)	Solvent	Experimental Data[a]			Fitted Values	
		C_∞	γ_D	N_A	D_∞/D_o	N_A
25	Benzene	0.0581	79.01	1.1908	103.17	1.235
	Toluene	0.0523	88.24	0.7897	105.20	0.8157
	Chlorobenzene	0.0704	73.31	1.4061	180.20	1.4439
45	Benzene	0.0648	62.66	22.376	57.3	22.569
	Toluene	0.0569	80.20	11.368	95.4	11.320
	Chlorobenzene	0.0771	54.55	22.504	71.02	23.533
65	Benzene	0.0843	51.03	296.91[b]	78.71	311.92
	Toluene	0.0690	61.44	135.37[b]	72.25	139.73
	Chlorobenzene	0.0892	47.08	210.27[b]	67.00	211.12

[a] Units: C_∞ (g/cm^3), N_A (g/m^2 · day), γ_D (cm^3/g).
[b] Denotes that the value was abstracted from Arrhenius relationship of permeation rate versus inverse temperature.

Table VIII Fitted Parameters for Repeated Sorption Experiments with ECTFE (cf. Table VI)

Solvent (Temperature)	Parameter	Fitted Parameter Values		
		Fresh Sample	1st Exposure	2nd Exposure
Benzene (25°C)	α	0.656	0.816	
	$D_F \times 10^4$	0.207	0.389	
	k_{fo}	0.0325	0.052	
	γ_k	90	90	
Toluene (45°C)	α	0.734	0.618	0.543
	$D_F \times 10^4$	3.45	1.13	0.680
	k_{fo}	0.609	0.408	0.256
	γ_k	76	77	72

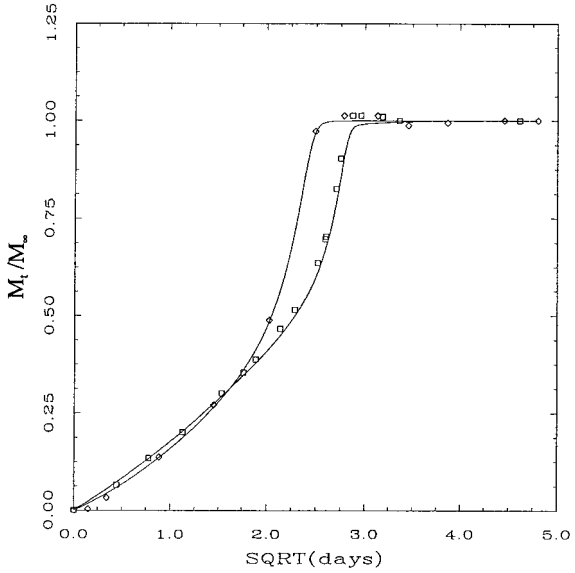

Figure 9 The fitted curves of presorbed ECTFE sample by benzene at 25°C. (□) fresh sample, (◇) presorbed sample.

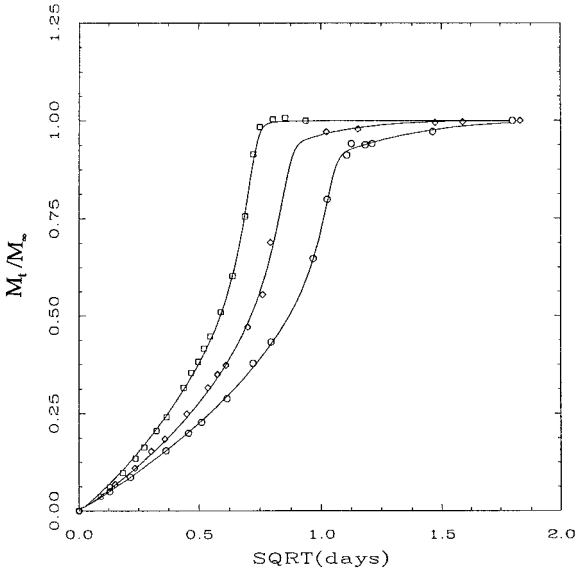

Figure 10 The fitted curves of repeatedly exposed ECTFE samples by toluene at 45°C. (□) fresh sample, (◇) first exposed sample, (○) second exposed sample.

energies for the relaxation rate coefficient, k_{fo}, and the initial diffusivity, D_o, were in the range of 3–4 and 0.5–1.5 kcal/mol, respectively. The value at 25°C was fitted to the rate equations and was found to be in the range of 10^{-11}–10^{-12} cm^2/sec, which is typical of glassy polymers. In addition, the predicted diffusivity in PVDF decreased as the size of the penetrant increased. In ECTFE, the predicted diffusivity of benzene is the highest among the penetrants, regardless of temperature.

Stress-Strain Tests

The action of solvents on polymers is in many ways similar to that of plasticizers. Solvents can form secondary bonds to the polymer chains, and they can penetrate and replace the interchain secondary bonds, and thereby pull apart and dissolve linear and branched polymers. Deformation of the polymer below the yield point (in the elastic region) is most important because the plasticizing effect is predominantly exhibited in this elastic region.

Table IX Fitted Rate Parameters for Sorption Rate Experiments via Eq. (15) for Various Penetrants in PVDF

Temperature (°C)	Parameter	Fitted Parameter Values of PVDF		
		Benzene	Toluene	Chlorobenzene
25	α	0.699	0.672	0.756
	$D_o \times 10^4$	0.016	0.011	0.006
	k_{fo}	0.013	0.006	0.011
	D_∞/D_o	27.84	35.09	12.12
45	α	0.725	0.766	0.787
	$D_o \times 10^4$	0.280	0.162	0.095
	k_{fo}	0.174	0.148	0.208
	D_∞/D_o	21.12	15.11	8.300
65	α	0.650	0.742	0.743
	$D_o \times 10^4$	1.915	0.973	0.806
	k_{fo}	1.200	1.257	1.220
	D_∞/D_o	25.46	13.00	9.128

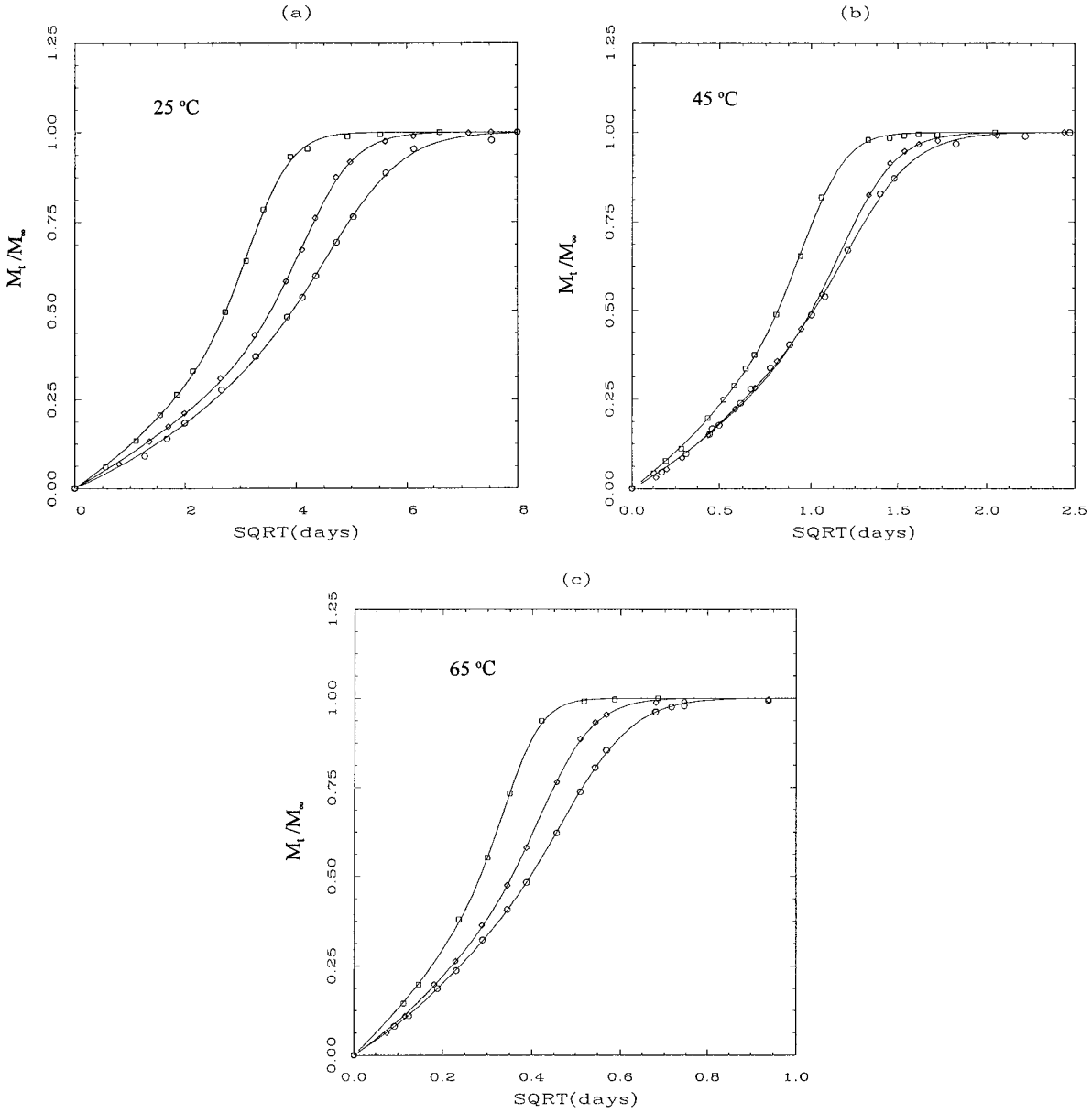

Figure 11 The fitted data of PVDF with aromatic liquid sorption at 25, 45, and 65°C by a quadratic type of rate equation. (□) benzene, (◇) toluene, (○) chlorobenzene.

Polymer Types

PFA, FEP, or ETFE do not exhibit distinct yield points at room temperature, even without being exposed to penetrants. ETFE exhibited higher tensile strength than both PFA and FEP resins. A barely noticeable flat inflection point exists early in the tensile test of a fresh ETFE sample, and the slope in this elastic region is quite steep. Subsequent exposure to solvents had little or no effect on their stress-strain curves. They maintained structural integrity, although a slight change of mechanical properties occurred [see Fig. 14(a–c)]. After immersion, however, ETFE exhibited a more gradual transition between the initial elastic and draw regions. These observations agreed with the fact that their transport properties showed little effect of relaxation.

On the other hand, PVDF and ECTFE exhibit tensile stress-strain diagrams that are more typical of semicrystalline polymers. Furthermore, PVDF has the highest tensile strength of the fluoropolymers tested. Impregnated samples of PVDF exhibited slight decreases of yield stress

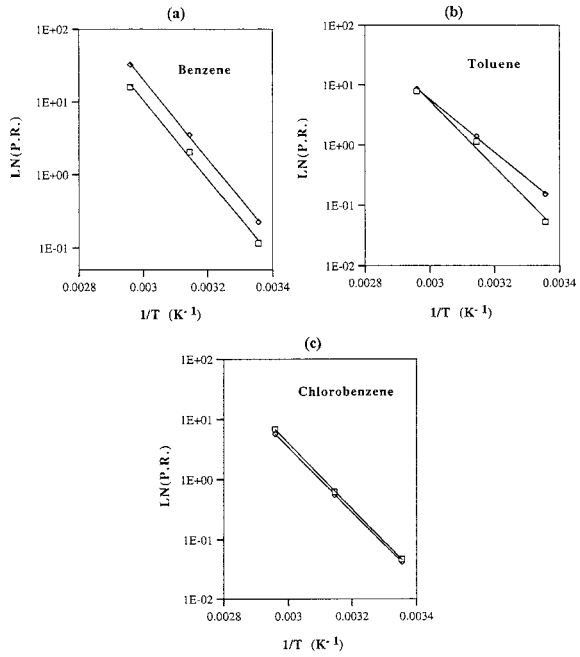

Figure 12 The comparison of calculated permeation rates from the kinetic model with experimental data from PVDF-penetrant systems. (□) experimental, (◇) calculated.

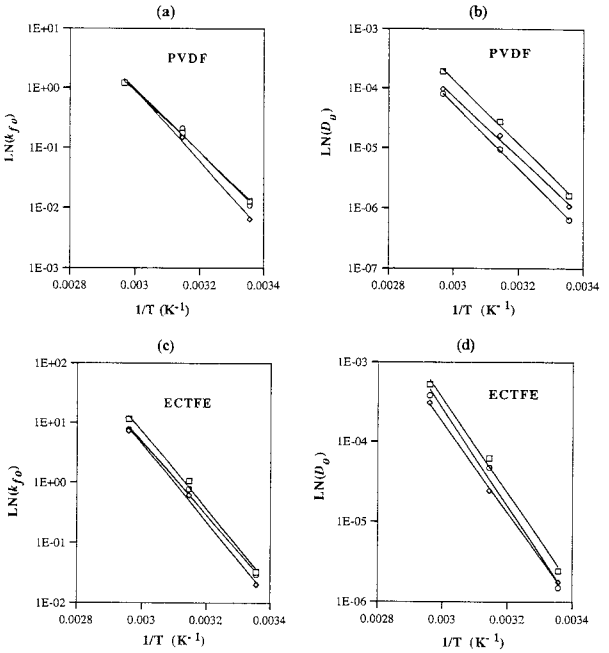

Figure 13 The Arrhenius plot of diffusivity and rate coefficient obtained from fitting PVDF and ECTFE sorption data.

but slight increases of the elastic strain, as shown in Figure 14(d) and (e). It exhibited widely varied responses to immersion in the solvents, especially for MEK, as shown in Figure 15. The yield point practically disappeared in machine-oriented (MO) PVDF, and for transverse-oriented (TO) PVDF, it became less distinct. The yield stress was reduced by about 25%, and the elastic strain was increased by a factor of 3–4, as shown in Table XI. This behavior coincides with the very steep sorption curve of the PVDF-MEK system, indicating a high degree of plasticization. Oddly, the yield point for MO samples of impregnated ECTFE also vanished, and the tensile strength changed more smoothly as strain increased. In contrast, for TO ECTFE, a significant change of stress-strain diagram was also observed: the yield stress dropped by ~ 50%, but the strain at the yield point increased by >100% [see Fig. 14(f) and (g)]. For ECTFE, the effects of the chemicals tested here were almost identical, as shown in Figure 15. This observation is consistent with the

Table X Calculated Permeation Rates from Fitted Parameters of the Quadratic Rate Equation and Experimental Values for Various Penetrants in PVDF

Temperature (°C)	Penetrant Type	C_∞ (g/cm^3)	Permeation Rate (g/m^2·day)	
			Experimental	Predicted
25	Benzene	0.0437	0.115	0.225
	Toluene	0.0373	0.053	0.152
	Chlorobenzene	0.0375	0.047	0.042
45	Benzene	0.0484	2.054	3.510
	Toluene	0.0417	1.134	1.383
	Chlorobenzene	0.0427	0.627	0.553
65	Benzene	0.0569	15.958	32.431
	Toluene	0.0475	7.862	8.513
	Chlorobenzene	0.0491	6.921	5.732

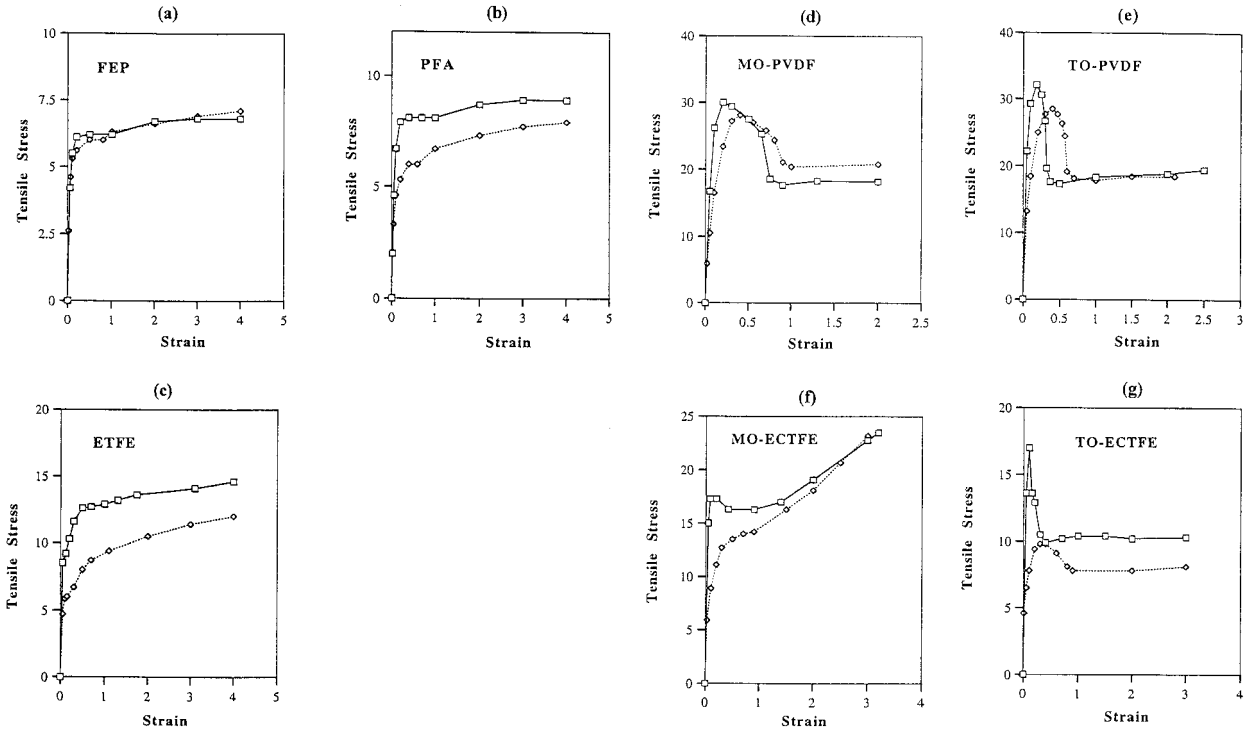

Figure 14 Stress-strain curves of impregnated fluoropolymers by toluene. (□) fresh sample, (◇) exposed sample.

almost identical shapes of the sorption curves for ECTFE, irrespective of the solvent type.

CONCLUSIONS

Fluoropolymer sheets of varying thicknesses that were exposed to various liquid- and vapor-phase penetrants at several temperatures and concentrations exhibited a broad range of sorption behavior, from classic Fickian diffusion to anomalous sorption. Fully fluorinated polymers tended to exhibit Fickian diffusion, while partially fluorinated polymers produced various anomalous sorption responses. The latter responses diverged from normal Fickian sorption, in the following order: ETFE → PVDF → ECTFE. The main cause of that behavior seems to arise from polar interchain attractions caused by substituent elements. From several sets of experimental results, it was concluded that the intersegmental bonds of PVDF are likely to be protonic, and those of ECTFE are much like dipole-dipole interactions. To the contrary, ETFE is less polar than ECTFE and less protonic than PVDF.

The increase of polar intersegmental attraction produced a high cohesive energy density and resulted in good mechanical properties. A collateral result was, however, that non-Fickian diffusion was induced by the relaxation-controlled disruption of polar intersegmental bonds, apparently caused by solvent plasticization. That eventually led to the creation of free volume at a rate that was dependent on both time and concentration, which led to time dependence of both solubility and diffusivity because they depend on free volume.

From stress-strain tests, it was confirmed that modified fluoropolymers (PVDF, ECTFE, and ETFE) have higher yield stress and tensile strength than perfluorinated resins (FEP and PFA). Furthermore, the observed non-Fickian diffusion behavior was closely related to the change of the mechanical properties of the corresponding polymers between the virgin and impregnated states. For polymers that exhibited Fickian transport (e.g., FEP, PFA, and ETFE), the change of mechanical properties was not significant. Conversely, for polymers that exhibited non-Fickian transport (e.g., PVDF and ECTFE), drastic changes of mechanical properties were ob-

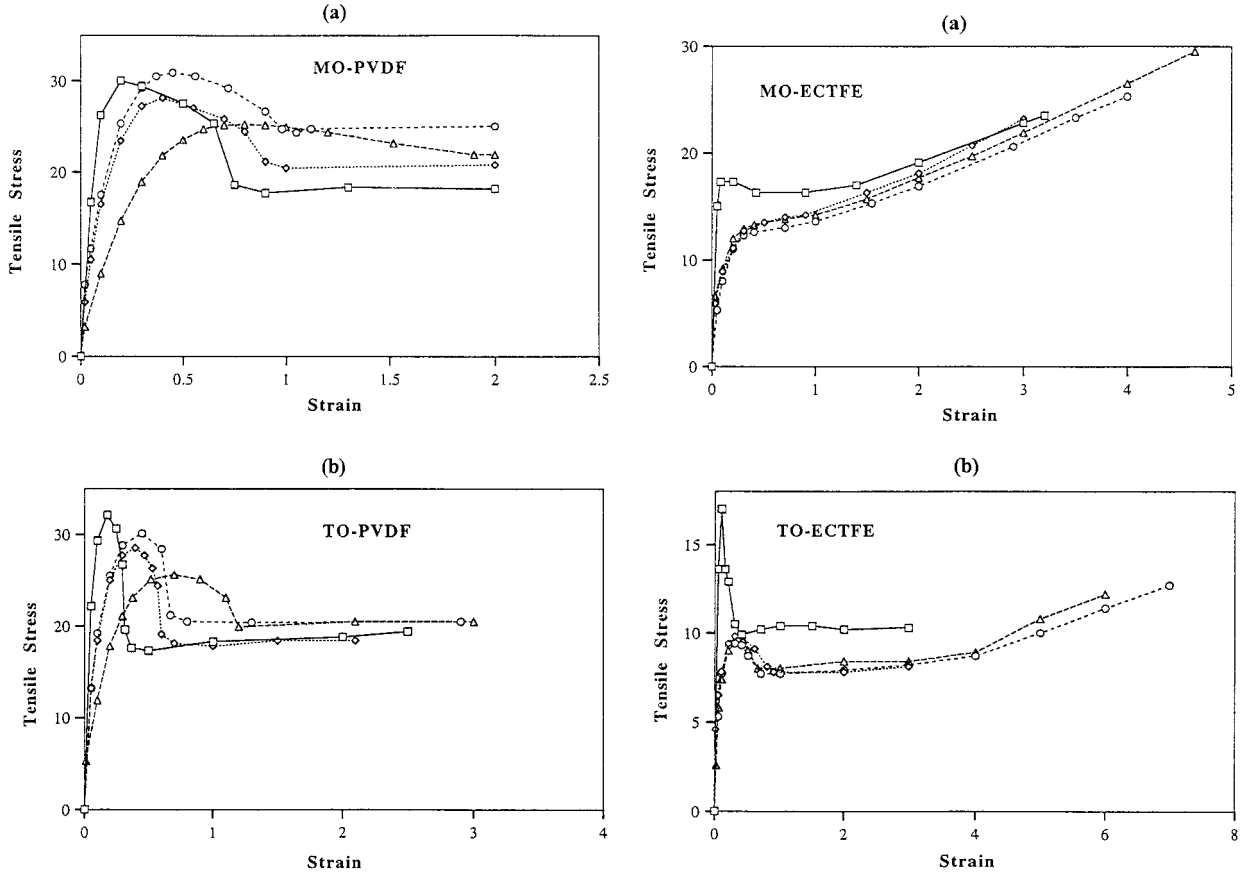

Figure 15 Tensile stress-strain curves of PVDF with various organic chemicals. (□) no solvent, (◇) toluene, (○) dichloromethane, (△) MEK.

served. Notably, the shapes of sorption curves were strongly related to the degree of deformation of the polymer structure.

For example, neither the sorption curves nor the stress-strain diagrams of ECTFE were affected by solvent type. For MO samples, the yield

Table XI The Tensile Properties of Virgin (Unsorbed) and Impregnated (Sorbed) Fluoropolymers[a]

Polymer	Mechanical Property	No Solvent	$C_6H_5CH_3$	C_6H_5Cl	CH_2Cl_2	$CH_3COC_2H_5$
FEP	Elastic strain	No yield	No yield	No yield	No yield	No yield
PFA	Yield stress					
ETFE	Elastic strain	0.072	No yield	No yield	No yield	No yield
	Yield stress	8.4				
ECTFE	Elastic strain	0.09	No yield	No yield	No yield	No yield
(machine)	Yield stress	17.1				
ECTFE	Elastic strain	0.10	0.30	0.33	0.3	0.32
(transverse)	Yield stress	17.0	9.0	9.4	9.4	8.3
PVDF	Elastic strain	0.22	0.38	0.39	0.45	0.8
(machine)	Yield stress	29.7	28.8	26.4	23.5	25.5
PVDF	Elastic strain	0.18	0.39	0.34	0.4	0.67
(transverse)	Yield stress	32.0	28.5	28.1	24.3	25.6

[a] Units: tensile stress (lb_f), elastic strain (inch). Elastic strain indicates the strain at yield point, and yield stress represents the force (or tensile stress) at the yield point. "No yield" denotes "no apparent yield point."

point disappeared, and for TO samples, the yield stress decreased by 50% of the original value, but the stress at the yield point increased by approximately 300%.

On the other hand, the shapes of sorption curves for PVDF exhibited different degrees of sorption anomalies for different solvents, corresponding to their ability to alter the structure. That is, weak swelling agents exhibited nearly Fickian transport, and strong swelling agents exhibited anomalous diffusion. Impregnated samples exhibited slight decreases of yield stress and increases of the elastic strain up to 100%. For highly plasticizing solvents (e.g., MEK), the yield point became ambiguous and the elastic strain was increased by a factor of 3–4.

Finally, a kinetic model was devised to interpret the observed anomalies for PVDF and ECTFE. It represented quadratic and exponential dependence of diffusivity on relaxation under slightly different assumptions. The theoretical results obtained from rate equations have described observations of anomalous sorption behavior in a consistent manner for both transient sorption and steady-state permeation. In addition, the physical parameters from both types of equations gave reasonable values and followed the expected general trends of temperature dependence. For example, the initial diffusivity, D_0 at 25°C, ranged from 10^{-11} to 10^{-12}, which is typical of glassy polymers. In addition, the initial diffusivity increased as the size of the penetrant decreased. The extracted rate parameters, D_0 and k_{fo}, exhibited Arrhenius temperature dependence. The parameters deduced from transient sorption data were used to predict permeation rates, and the results agreed with independently measured values within an order of magnitude. Despite some discrepancies, anomalous sorption behavior in the glass transition range could be described solely on the basis of volume relaxation kinetics. That provided evidence that the model and parameters are valid over the ranges studied.

The work reported here was conducted at Ohio State University. The authors are grateful for the use of the facilities and generosity. Financial support provided for part of this study and the contribution of the polymer samples used in this study by E. I. du Pont de Nemours & Co. are gratefully acknowledged. In addition, many helpful suggestions were made by Dr. Sina Ebnesajjad.

REFERENCES

1. R. J. Plunkett, U. S. Pat. 2,230,654 (Feb. 4, 1941) (to Kinetic Chemicals, Inc.).
2. "Fluoropolymers," in *Encyclopedia of Polymer Science and Engineering,* Wiley, New York, 1986, Vol. 16.
3. "DuPont Polymers for the Chemical Processing Industry," DuPont, H-42451, 1992.
4. "Halar™—Polyvinylidene Fluoride," Ausimont USA, Inc., AUS-0021, April 1991.
5. "Halar® ECTFE Fluoropolymer," Ausimont USA, Inc., 1995.
6. "Kynar®," Spotlight, Elf Ato Chem, May 1991, Vol. 19, No. 1.
7. "The New Breeds," *Plastics Technology,* **37,** 58 (1991).
8. C. W. Bunn, *J. Polym. Sci.,* **16,** 332 (1955).
9. E. S. Clark, paper presented at Symposium on Helices in Macromolecular Systems, Polytechnic Institute of Brooklyn, Brooklyn, NY, May 16, 1959.
10. Y. Miamoto, H. Miyah, and K. J. Asai, *J. Polym. Sci. Polym. Phys. Ed.,* **18,** 597 (1980).
11. M. Fujji, V. Stannett, and H. B. Hopfenberg, *J. Macromol. Sci. Phys.,* **B15,** 421 (1978).
12. C. E. Rogers, in *Polymer Permeability,* J. Comyn, Ed., Elsevier, London, 1985, Chap. 2.
13. J. Crank and G. S. Park, *Diffusion in Polymers,* Academic Press, London, 1968.
14. J. Crank, *The Mathematics of Diffusion,* Oxford University Press, Oxford, 1975, 2nd Ed.
15. W. Ostwald, *Z. Physik. Chem.,* **111A,** 62 (1924).
16. C. E. Rogers, in *Physics and Chemistry of the Organic Solid State,* D. Fox, M. M. Labes, and A. Weissberger, Eds., Interscience Publ., New York, 1965, Vol. II, Chap. 6.
17. G. S. Park, *Trans. Faraday Soc.,* **48,** 11 (1952).
18. F. A. Long and R. J. Kokes, *J. Am. Chem. Soc.,* **75,** 2232 (1953).
19. A. C. Newns, *Trans. Faraday Soc.,* **52,** 1533 (1956).
20. F. A. Long and D. Richman, *J. Am. Chem. Soc.,* **82,** 513 (1960).
21. E. Bagley and F. A. Long, *J. Am. Chem. Soc.,* **77,** 2172 (1955).
22. I. C. Wat, *Textile Res. J.,* **30,** 443, 644 (1960).
23. N. Overbergh, H. Berghmans, and G. Smets, *Polymer,* **16,** 703 (1975).
24. J. S. Vrentas, J. L. Duda, and A. C. Hou, *J. Appl. Polym. Sci.,* **29,** 399 (1984).
25. T. Alfrey, E. F. Gurnee, and W. G. Lloyd, *J. Polym. Sci. C,* **12,** 249 (1966).
26. H. B. Hopfenberg, V. T. Stannett, and G. M. Folk, *Polym. Eng. Sci.,* **15,** 261 (1975).
27. N. Thomas and A. H. Windle, *J. Memb. Sci.,* **3,** 337 (1978).
28. C. H. M. Jacques, H. B. Hopfenberg, and V. T.

Stannet, in *Permeability of Plastic Films and Coatings,* H. B. Hopfenberg, Ed., Plenum, New York, 1974.
29. C. Gostoli and G. C. Sarti, *Chem. Eng. Comm.,* **21,** 67 (1983).
30. H. L. Frish, *Polym. Eng. Sci.,* **20,** 2 (1980).
31. S. W. Lee and K. S. Knaebel, *AIChE J.,* to appear.
32. A. R. Berens and H. B. Hopfenberg, *Polymer,* **19,** 489 (1978).
33. A. K. Doolittle, *J. Appl. Phys.,* **22,** 1471 (1951).
34. M. L. Williams, R. F. Landel, and J. D. Ferry, *J. Am. Chem. Soc.,* **77,** 3701 (1955).
35. H. Fujita, *Fortschr. Hochpolym. Forsch,* **3,** 1 (1961).
36. S. A. Stern and S. Kulkarni, *J. Polym. Sci.,* **21,** 441 (1983).
37. S. W. Lee and K. S. Knaebel, *J. Appl. Polym. Sci.,* to appear.
38. A. Peterlin, *Mechanism of Deformation in Polymeric Solids in Polymeric Materials,* Eric Baer, Ed., Metals Park, Ohio, 1973.
39. H. L. Thomas and A. H. Windle, *Polymer,* **21,** 613 (1980).
40. L. Nicolais, E. Drioli, H. B. Hopfenberg, and D. Tidone, *Polymer,* **18,** 1137 (1977).
41. L. Nicolais, E. Drioli, H. B. Hopfenberg, and G. Caricati, *J. Memb. Sci.,* **3,** 231 (1978).